

SYNTHESIS OF LITHIUM TITANATE ($\text{Li}_4\text{Ti}_5\text{O}_{12}$) BY ADDITION OF EXCESS LITHIUM CARBONATE (Li_2CO_3) IN TITANIUM DIOXIDE (TiO_2) XEROGEL

Anne Zulfia Syahrial¹, Bambang Priyono^{1*}, Akhmad Herman Yuwono¹, Evvy Kartini², Heri Jodi², Johansyah¹

¹ *Department of Metallurgy and Materials Engineering, Faculty of Engineering, Universitas Indonesia, Kampus UI Depok, Depok 16424, Indonesia*

² *Center for Science and Technology of Advanced Materials, BATAN, Puspitak Serpong, Indonesia*

(Received: December 2015 / Revised: January 2016 / Accepted: February 2016)

ABSTRACT

Lithium titanate, $\text{Li}_4\text{Ti}_5\text{O}_{12}$ (LTO) is a promising candidate as lithium ion battery anode material. In this investigation, LTO was synthesized by a solid state method using TiO_2 xerogel prepared by the sol-gel method and lithium carbonate (Li_2CO_3). Three variations of Li_2CO_3 content addition in mol% or Li_2CO_3 molar excess were fabricated, i.e., 0, 50 and 100%, labelled as sample LTO-1, LTO-2 and LTO-3, respectively. The characterizations were made using XRD, FESEM, and BET testing. These were performed to observe the effect of lithium excess addition on structure, morphology, and surface area of the resulting samples. Results showed that the crystallite size and surface area of each sample was 50.80 nm, 17.86 m²/gr for LTO-1; 53.14 nm, 22.53 m²/gr for LTO-2; and 38.09 nm, 16.80 m²/gr for LTO-3. Furthermore, lithium excess caused the formation of impure compound Li_2TiO_3 , while a very small amount of rutile TiO_2 was found in LTO-1. A near-pure crystalline $\text{Li}_4\text{Ti}_5\text{O}_{12}$ compound was successfully synthesized using the present method with stoichiometric composition with 0% excess, indicating very little Li^+ loss during the sintering process.

Keywords: Excess lithium carbonat; Lithium titanate ($\text{Li}_4\text{Ti}_5\text{O}_{12}$); Sintering; Solid-state; Xerogel

1. INTRODUCTION

To overcome the energy crisis and environmental pollution, renewable energy sources have been developed to supply power for electric vehicles with zero emissions. Electric vehicles create additional economic development opportunities by improving quality of life, reducing energy cost and decreasing reliance on foreign oil (Todd, 2013). One component of the electric car that is absolutely necessary is a rechargeable battery, and the lithium ion battery (LIB) is most widely used for this purpose today. The LIB generally uses graphite as anode material. However, compared to graphite, lithium titanate ($\text{Li}_4\text{Ti}_5\text{O}_{12}$ or LTO) offers more advantages. LTO is known as a zero-strain insertion oxide that can undergo thousands of cycles with little capacity loss. Additionally, its insertion potential (1.55 V vs. Li/Li+) remains above the onset of Solid Electrolyte Interphase (SEI) formation, taking advantage of nano-scale features that are not normally feasible with carbon electrodes due to excessive SEI (Solid Electrolyte Interface) buildup (Maloney et al., 2012). Further, the electrochemical characteristics of the LTO compound prove that LTO has the potential for electrochemical reaction kinetics leading to an

*Corresponding author's email: bambang.priyono@ui.ac.id, Tel. +62-21-7863510, Fax. +62-21-7872350
Permalink/DOI: <http://dx.doi.org/10.14716/ijtech.v7i3.2890>

excellent capability rate and stabile cycling performance (Li & Mao, 2014).

Although LTO has many desirable properties, this material has low electrical conductivity, requiring modification of the material structure for use in high current applications. Thus, although LTO has a theoretical specific capacity of 175 mAh/g, the ability to provide charge/discharge currents are relatively low because of large polarization due to the low electrical conductivity (Rho & Kanamura, 2004) and slow lithium ion (Li-ion) diffusion (Ouyang et al., 2007). Efforts to enhance LTO conductivity include doping with other elements and coating with more conductive materials (Park et al., 2008). The ionic diffusion of ion Li^+ is increased by reducing particle size to increase the surface contact between electrodes and electrolytes, also reducing diffusion of the Li-ion and electron paths to enhance lithiation kinetics (Zhang et al., 2013).

The sol-gel procedure has been applied extensively to synthesize nanoparticles by controlling the reaction at the molecular level, obtaining nanoparticles with high homogeneity (Bilecka & Niederberger, 2010). The product resulted from sol-gel processing a higher surface area than the solid-state process (Priyono et al., 2013). Further, the sintering temperature required to form spinel-crystalline is significantly lower than the solid-state method (Zhang et al., 2013). In this research, the LTO anode was made using the sol-gel process to prepare TiO_2 xerogel, calcined to form the TiO_2 -anatase phase and mixed with lithium carbonate to form LTO upon sintering at 750°C . It aims to obtain LTO with nano-crystalline structure and high surface area. By using lithium carbonate (Li_2CO_3) as the Li-ion source (Mandal et al., 2012), the formation of LTO will release CO_2 gas and leave an empty space for creating an enhanced porous structure.

2. EXPERIMENTAL METHOD

LTO powder was synthesized by the sol-gel method using titanium tetra-*n*-butoxide (Kanto Chemical) to prepare TiO_2 xerogel, and calcined to obtain TiO_2 anatase. Then, lithium carbonate pa. (pro analysis) grade was mixed with synthesized TiO_2 anatase and subsequently sintered to obtain LTO. The procedure used to obtain TiO_2 xerogel was explained by Priyono et al. (2013).

To obtain crystalline anatase of the TiO_2 xerogel, two stages of calcination were carried out. The first step was conducted at 150°C for three hours to evaporate the solvent, and the second step was carried out at 300°C for three hours to remove the remaining organic compounds and formation of TiO_2 anatase. It should be noted that the first step was performed under inert atmosphere, while the final step was accomplished under air flow to oxidize the carbon in the remaining organic compound and obtain the white powder TiO_2 anatase.

In the next step, to obtain LTO, mixing TiO_2 anatase and Li_2CO_3 in solid state processing was carried out by using a high energy ball mill at 2,000 rpm for two hours, and continued with the sintering process at 750°C with time to rise the temperature (rising time) for two hours and holding time for one hour. The off-white LTO powder was collected for further analysis. The sample of LTO-1 denotes 0% mol Li_2CO_3 excess or in stoichiometric ratio, LTO-2 denotes 50% mol Li_2CO_3 excess and LTO-3 denotes 100% mol Li_2CO_3 excess. The use of such Li_2CO_3 excess in solid state mixing is to anticipate the superfluous loss of Li-ion during sintering process.

The characterization by x-ray diffraction (XRD) was carried out to identify the crystal structure of each solid sample obtained and the final lithium titanate. The crystallite size was estimated based on XRD data via Scherrer's equation analysis. Further, the Brunauer-Emmet-Teller (BET) measurement (Quantachrome NOVA 1200e) was used to determine the surface area of the sample. Energy Dispersive Spectroscopy (EDS) testing was conducted to determine the Ti and O atomic compositions of TiO_2 xerogel. Further, Field Emission Scanning Electrone Microscopy (FESEM) analysis was performed to identify morphology structure on the surface

and particle size of LTO. Finally, conductivity and impedance testing was carried out using HIOKI LCR-Meter to obtain impedance and conductivity characteristics of the solid. As a comparison, LTO obtained through the courtesy of the Korean Institute of Science and Technology (KIST) was used in this research as reference LTO.

3. RESULTS AND DISCUSSION

3.1. Formation of Anatase TiO_2 Xerogel

The atomic composition of TiO_2 xerogel after calcination at 300°C for two hours as determined by EDS is shown in Table 1.

Table 1 EDS result of TiO_2 xerogel in three spots

Spot	Weight Percent (% wt)		Atomic Percent (%at)	
	Ti	O	Ti	O
1	63.83	36.17	37.08	62.95
2	58.71	41.29	32.20	67.80
3	64.46	35.54	37.73	62.27
Average	62.33	37.66	35.67	64.34

Further, the spots of EDS testing are depicted in Figure 1, as follows:

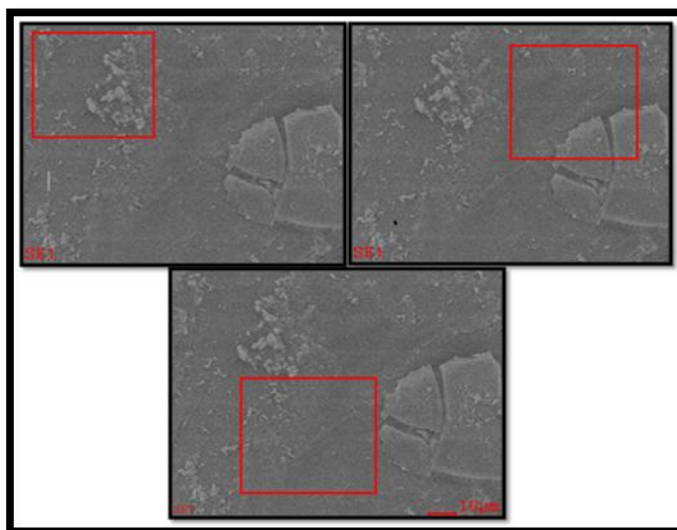


Figure 1 Spots of EDS testing

EDS composition testing is required to ensure the purity of the starting material used to manufacture LTO. All organic and volatile matters contained in the xerogel disappeared upon the calcination process. No other major element was detected in the result. From Table 1, the average percentage ratio of moles Ti:O is 1:1.8, while the stoichiometric ratio $\text{Ti:O} = 1:2$. This may be caused by a lack of oxygen supply during the calcination process. However, it may be said that the composition is indeed TiO_2 . To confirm this result, XRD testing was performed to check the sample and its crystallinity following the calcination process. The diffraction pattern of TiO_2 anatase is shown in Figure 2.

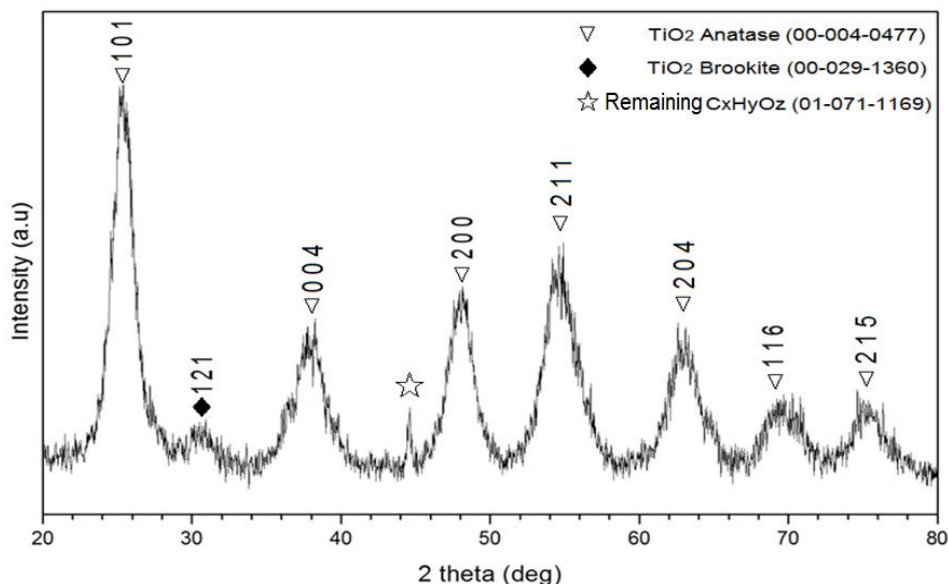


Figure 2 X Ray-diffraction pattern of TiO_2 xerogel calcined at 300°C

Prior to calcination, xerogel has an amorphous structure (Priyono et al., 2013), while after calcination at 300°C , the peaks as shown in Figure 2 belonging to TiO_2 anatase are observed in the XRD-pattern (JCPDS ref. code: 00-004-0477-anatase synthetic). However, the small peaks of TiO_2 Brookite (JCPDS ref. code: 00-029-1360) and the remaining $\text{C}_x\text{H}_y\text{O}_z$ (JCPDS ref. code: 01-071-1169) were detected. It is important to know the crystalline structure of TiO_2 anatase prevailed at 300°C calcination. Since this solid TiO_2 was produced using the sol-gel method, the lowest possible calcination is desired to preserve the surface area. The average crystallite size was calculated by full width at half maximum (FWHM) of the XRD 2θ peaks using the Scherrer equation and result was 7.62 nm.

3.2. Sintering Leads to LTO Spinel Formation

The XRD pattern of post-sintering solids, together with the LTO reference from the KIST, are shown in Figure 3. Figure 3 shows the XRD patterns of LTO resulting from the sintering process at 750°C . All LTO-1 and LTO-2 samples show the dominant lithium titanate spinel crystalline structure (JCPDS: 00-049-0207). The peaks were detected at 35.57° , 43.24° , 57.21° , 62.83° , 66.07° , 74.34° , 79.34° and 82.37° . The only differences between LTO-1 and LTO-2 were the impurities contained, as detected from the above XRD-Pattern, i.e., the stronger peak of Li_2TiO_3 resulting from increasing the content Li ion source in LTO-2. Further, the XRD patterns match with the structure of LTO from KIST. Thus, in this research, the LTO anode material with spinel structure has been successfully synthesized. Additionally, both LTO-1 and LTO-2 contain lithium hydride (JCPDS: 01-078-0840) as the impurity with the same peak intensity. The presence of lithium hydride might be caused by improper preparation and the sintering process.

In Figure 3, the XRD pattern of LTO-1 shows two peaks of TiO_2 rutile at 27.46° and 53.34° (JCPDS: 00-004-0551) at very low intensity and a peak of Li_2TiO_3 at 43.72° (JCPDS: 00-033-0831), also at very low intensity.

The impurity of TiO_2 rutile was formed by unreacted TiO_2 anatase during the formation of LTO. However, the existence of Li_2TiO_3 peaks indicate that the unreacted TiO_2 anatase was caused not only by loss of the Li^+ ion source during the sintering process, but also by inhomogeneous mixture during the solid state mixing process. Further, the very low intensity of

Li_2TiO_3 and TiO_2 rutile peaks at the stoichiometric composition indicates that there was little loss of the Li-ion source during the sintering process.

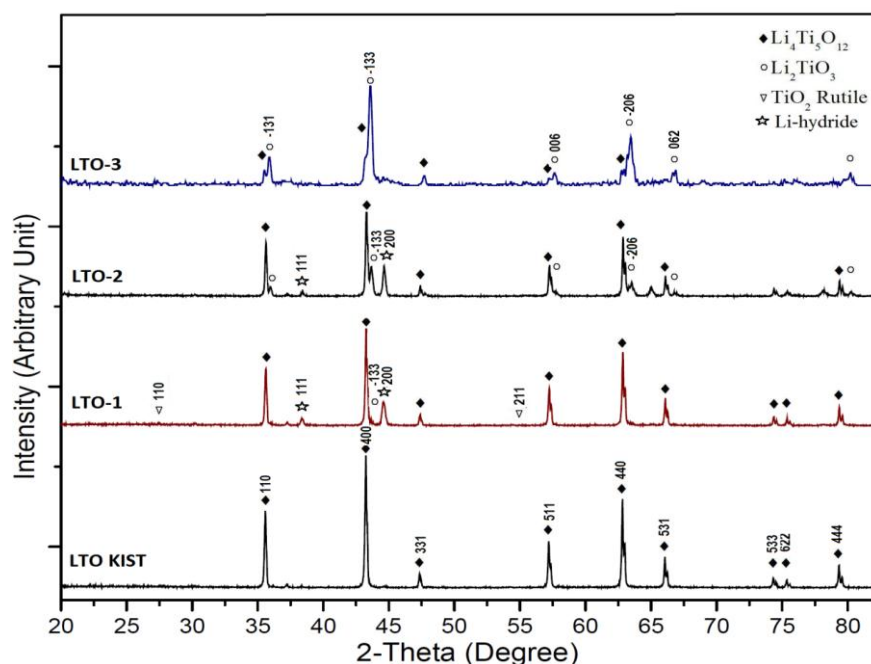


Figure 3 X Ray-diffraction pattern of LTO-1, LTO-2 sintered at 750°C and LTO from KIST

Still, in Figure 3, the XRD pattern of LTO-2 shows two peaks of Li_2TiO_3 at 43.58 and 43.72 (JCPDS: 00-033-0831) at stronger intensity than LTO-1, with no TiO_2 rutile peak. This indicates that all TiO_2 anatase reacted with the Li^+ ion source during the sintering process and the excess of Li^+ ion source lead to the formation of more Li_2TiO_3 , which has a Li/Ti molar ratio higher than $\text{Li}_4\text{Ti}_5\text{O}_{12}$ (Yoshikawa et al. 2010). Further, the XRD pattern of LTO-3 shows that the Li_2TiO_3 peaks became more dominant than $\text{Li}_4\text{Ti}_5\text{O}_{12}$ peaks.

The TiO_2 rutile and Li_2TiO_3 formed may be disadvantageous for lithium ion diffusion (Yoshikawa et al. 2010). Thus, it is desirable to obtain a high purity LTO/ $\text{Li}_4\text{Ti}_5\text{O}_{12}$. Nevertheless, TiO_2 rutile has the capacity of 270 mAh/g, which is higher than LTO (175 mAh/g) as reported by Sun et al. (2014). There is an effort to make an *in situ* synthesized $\text{Li}_4\text{Ti}_5\text{O}_{12}$ /rutile- TiO_2 composite (Li & Mao, 2014).

The average crystallite size of the solids estimated using the Scherrer equation with fit size fit size analysis (Speakman, 2015) is presented in Table 2. All solids obtained have a crystallite size of well below 100 nm as a benchmark of the nanocrystalline size product.

Table 2 Average crystallite size diameter

Sample	Crystallite size (nm)
LTO-1	50.80
LTO-2	53.14
LTO-3	38.09
LTO KIST	48.47

Table 3 BET surface area result

Sample	Surface Area (m^2/gr)
LTO-1	17.86
LTO-2	22.52
LTO-3	16.80
LTO KIST	33.45

The TiO_2 anatase prepared by the sol-gel method seems to be an acceptable starting material to

produce LTO, and the 750°C sintering temperature is sufficient to form the LTO/spinel crystalline, which is lower than using TiO₂ anatase prepared using the solid state method, as reported by Shin et al. (2012).

3.3. BET Surface Area Result

The total capacity of the installed IPFC is required for solving the overload on the transmission. The TiO₂ xerogel calcined at 300°C had a surface area of 136.49 m²/g, which is higher than the other xerogel calcined at 420°C (Priyono et al., 2013). Additionally, compared to commercial TiO₂ from Merck (10 m²/g) (Augugliaro et al., 2005) and TiO₂ from Sigma (18.75 m²/g) (Ruslimie et al., 2011), the TiO₂ xerogel resulting from this sol-gel process had a significantly higher surface area. The sol-gel method could synthesize solid material with a high surface area (Wen, 2012). Thus, the present TiO₂ xerogel was a better prospective starting material for manufacturing high surface-area LTO.

Analogically, a high surface-area starting material must be used to obtain high surface-area LTO, since the subsequent heat treatment process to obtain the crystalline structure will cause agglomeration in the solid and reduce the surface area. In view of the foregoing, it is important to use the lower temperature process during calcination and sintering to preserve the surface area of the solid. The BET surface area testing of the sample of sintered product and the reference sample is presented in Table 3.

Table 3 shows the BET surface area of LTO-1, LTO-2, LTO-3 and LTO KIST. A large surface area is required to produce an LTO compound with a high capacity and cycle stability due to the large surface area, which will increase contact between the electrolytes and electrodes and shorten the diffusion paths for electrons and lithium ions (Zhang et al., 2013). It is interesting that the LTO obtained from the present research had a reasonably high surface area. This is a starting point for exploring the high surface area LTO for a high capacity anode.

3.4. Scanning Electron Microscopy Micrograph of Sintered Product

The Scanning Electron Microscopy (SEM) images of the sintered products LTO-1, LTO-2, LTO-3 and LTO KIST samples, respectively, are shown in Figure 5.

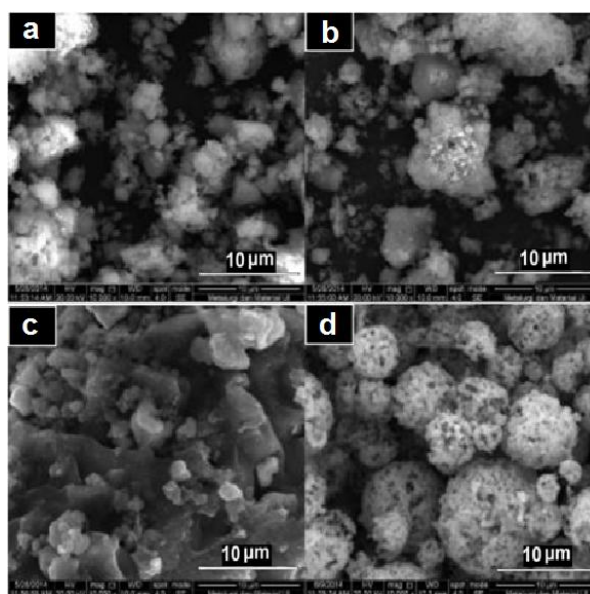


Figure 5 SEM images of: (a) LTO-1; (b) LTO-2; (c) LTO-3; (d) LTO from KIST

From Figure 5a, it can be seen that particles LTO-1 with mostly spherical shapes and sizes sticking together formed the agglomerate. Further, Figure 5b shows particles LTO-2 also

compose an agglomerate. The tiny particles that constitute the agglomerate still appear similar, with the size slightly larger than the LTO KIST shown in Figure 5d. Figure 5c shows particles LTO-3 have already formed a dense particulate, and the tiny particles forming the agglomerate are no longer visible. This causes a decrease in the surface area of LTO-3 compared to LTO-2. This large agglomerate of particles is thought to be a Li_2TiO_3 compound formed from the reaction between TiO_2 with excess lithium (Yoshikawa et al., 2010). Gu et al. (2014) reported that excess lithium leads to the formation of the Li_2TiO_3 compound. However, further research is needed to explain why the LTO-2 has a higher surface area than LTO-1 and LTO-3.

The magnificent image of Figure 5d shows the tiny particles of LTO KIST that compose the porous sphere agglomerate have a high level of homogeneity in size and shape. This structure leads to the highest surface area, compared to LTO-2 and LTO-3.

3.5. Impedance Measurement of Sintered LTO-1 and LTO KIST

Based on the XRD test, due to the closest relevance of the LTO-1 produced in this work compared to LTO KIST, both samples were measured for impedance to ascertain the conductivity of the solid materials. Figures 6A and 6B show the semicircular Nyquist plots of LTO-1 and LTO KIST, resulting from the conductivity and impedance testing that were carried out using a HIOKI LCR-Meter.

Figure 6A shows two semicircles for LTO-1, indicating several possibilities. Firstly, variance or non-uniformity of tiny particle size produced from the synthesis process as the result of sintering produces agglomerated particles with inhomogeneity of the particles, which then affects the resistivity of the bulk material. Secondly, the presence of impurities TiO_2 rutile and Li_2TiO_3 have different conductivity.

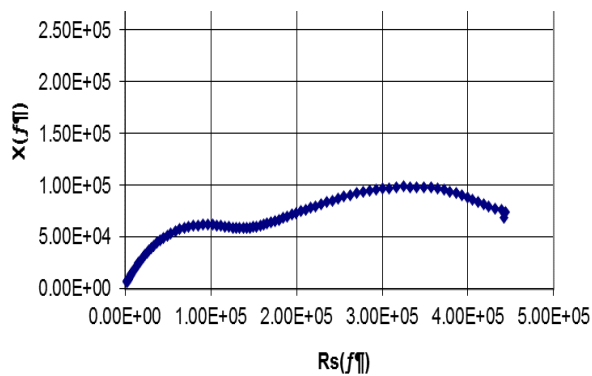


Figure 6A Nyquist plot of LTO-1

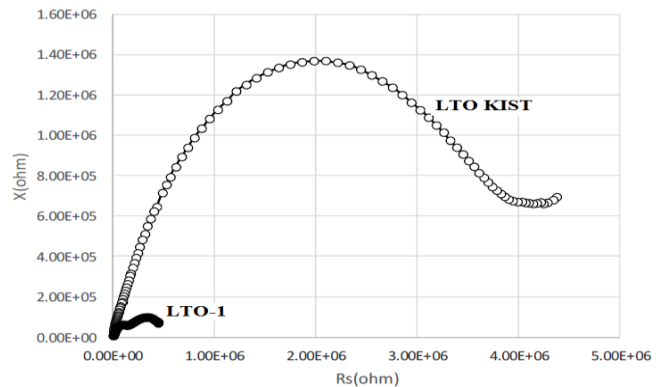


Figure 6B Nyquist plots of LTO-1 and LTO-KIST

Further, in Figure 6B, the Nyquist plot of LTO KIST shows one semicircle is much bigger than that of LTO-1. This indicates that LTO KIST has better homogeneity in particle morphology (as confirmed by SEM imaging) and fewer impurities (as supported by the XRD pattern). The larger Nyquist plot indicates that LTO-KIST has higher resistivity, as proved by conductivity calculations using regression of LCR equations.

To calculate conductivity, the conversion of impedance data and regression of the equation were obtained using the following conductivity equations:

$$\sigma_T = \sigma_{DC} + \sigma_{AC} \quad (1)$$

$$\text{since } \sigma_{AC} = A\omega^n \quad (2)$$

thus,

$$\sigma_T = \sigma_{DC} + A\omega^n \quad (3)$$

wherein

- σ_T : Overall conductivity (Siemens/cm)
- σ_{DC} : Direct Current (DC) conductivity
- σ_{AC} : Alternating Current (AC) conductivity

From the regression, it is obtained for LTO-1 by

$$\sigma_T = 9.92 \times 10^{-7} + 8.65 \times 10^{-11} \omega^{0.75} \text{ Siemen/cm}$$

while for LTO KIST, it is obtained by

$$\sigma_T = 1.53 \times 10^{-7} + 1.90 \times 10^{-11} \omega^{0.78} \text{ Siemen/cm}$$

Usually, conductivity data refers to DC conductivity, i.e.: 9.92×10^{-7} S/cm for LTO-1 and 1.53×10^{-7} S/cm for LTO KIST. From the said result, the conductivity of LTO-1 is higher than the conductivity of LTO KIST and the results were in line with LTO conductivity in the range of 10^{-7} S/cm, as reported by Young, et al. (Young et al., 2013). The conductivity of LTO-1 is higher than the reference LTO. However, this may be attributed to the existence of impurities that may have higher conductivity.

4. CONCLUSION

Lithium titanate, having quite a high surface area, was successfully synthesized using the sol-gel method with a calcination temperature of 300°C to form TiO₂ anatase, and with a sintering temperature of 750°C to obtain the Li₄Ti₅O₁₂ spinel structure. The XRD patterns show all structures were readily crystallized. The loss of the Li-ion source during processing is not superfluous, indicating that this TiO₂ xerogel and Li₂CO₃ mixture using high energy ball mill could promote the reaction needed to form Li₄Ti₅O₁₂ while preventing significant loss of the Li⁺ source.

The conductivity of LTO-1 obtained in this research was significantly higher than the reference LTO. Further, the influence of rutile TiO₂ existence and Li₂TiO₃ in the anode performance is interesting and should be studied in future research.

5. ACKNOWLEDGEMENT

The authors would like to thank the Riset Inovatif Produktif (RISPRO), Lembaga Pengelola Dana Pendidikan (LPDP), the Ministry of Finance of the Republic of Indonesia (contract number: SP1_012_B1_PM_Y/2014) for their financial support and Center for Science and Technology of Advanced Materials, Badan Tenaga Atom Nasional (BATAN), Puspiptek Serpong, Indonesia for the research facilities.

6. REFERENCES

- Augugliaro, V., Coluccia, S., García-López, E., Loddo, V., Marcì, G., Martra, G., Palmisano, L., Schiavello, M., 2005. Comparison of Different Photocatalytic Systems for Acetonitrile Degradation in Gas–solid Regime. *Topics in Catalysis*, Volume 35(3-4), pp. 237–244
- Bilecka, I., Niederberger, M., 2010. New Developments in the Nonaqueous and/or Non-hydrolytic Sol–gel Synthesis of Inorganic Nanoparticles. *Electrochimica Acta*, Volume 55(26), pp. 7717–7725
- Gu, Y.-J., Guo, Z., Liu, H.-Q., 2014. Structure and Electrochemical Properties of Li₄Ti₅O₁₂ with Li Excess as an Anode Electrode Material for Li-ion Batteries. *Electrochimica Acta*,

Volume 123, pp. 576–581

- Li, X., Mao, J., 2014. Sol-hydrothermal Synthesis of $\text{Li}_4\text{Ti}_5\text{O}_{12}$ /rutile- TiO_2 Composite as High Rate Anode Material for Lithium Ion Batteries. *Ceramics International*, Volume 40(8), pp. 13553–13558
- Maloney, R.P., Kim, H.J., Sakamoto, J.S., 2012. Lithium Titanate Aerogel for Advanced Lithium-ion Batteries. *Applied Material & Interfaces*, Volume 4, pp. 2318–2321
- Mandal, D., Sathiyamoorthy, D., Rao, V.G., 2012. Preparation and Characterization of Lithium-Titanate Pebbles by Solid-state Reaction Extrusion and Spherodization Techniques for Fusion Reactor. *Fusion Engineering and Design*, Volume 87, pp. 7–12
- Ouyang, C.Y., Zhong, Z.Y., Lei, M.S., 2007. Ab Initio Studies of Structural and Electronic Properties of $\text{Li}_4\text{Ti}_5\text{O}_{12}$ Spinel. *Electrochemistry Communications*, Volume 9(5), pp. 1107–1112
- Park, K., Benayad, A., Kang, D., Doo, S., 2008. Nitridation-driven Conductive $\text{Li}_4\text{Ti}_5\text{O}_{12}$ for Lithium Ion Batteries. *Journal of American Chemical Society Communication*, Volume 130(45), pp. 14930–14931
- Priyono, B., Yuwono, A.H., Munir, B., Rahman, A., Maulana, A., Abimanyu, H., 2013. Synthesis of Highly-ordered TiO_2 through CO_2 Supercritical Extraction for Dye-sensitized Solar Cell Application. *Advanced Materials Research*, Volume 789, pp. 28–32
- Rho, Y.H., Kanamura, K., 2004. Li^+ Ion Diffusion in $\text{Li}_4\text{Ti}_5\text{O}_{12}$ Thin Film Electrode Prepared by PVP Sol–gel Method. *Journal of Solid State Chemistry*, Volume 177(6), pp. 2094–2100
- Ruslimie, C.A., Razali, H., Khairul, W.M., 2011. Catalytic Study on TiO_2 Photocatalyst Synthesised via Microemulsion Method on Atrazine. *Sains Malaysiana*, Volume 40(8), pp. 897–902
- Shin, J.W., Chung, K.Y., Ryu, J.H., Park, I.W., Yoon, D.H., 2012. Effects of Li/Ti Ratios on the Electrochemical Properties of $\text{Li}_4\text{Ti}_5\text{O}_{12}$ Examined by Time-resolved X-ray Diffraction. *Applied Physics A*, Volume 107, pp. 769–775
- Speakman, S., 2015. *Estimating Crystallite Size Using XRD*, MIT Center for Materials Science and Engineering. Boston, Massachusetts, USA: MIT Center for Materials Science and Engineering. Available online at: <http://prism.mit.edu/xray/>, Accessed on 19 May 2015
- Sun, X., Radovanovic, P.V., Cui, B., 2014. Advances in Spinel $\text{Li}_4\text{Ti}_5\text{O}_{12}$ Anode Materials for Lithium-ion Batteries. *New Journal of Chemistry*, Volume 39, 38–63
- Todd, J., 2013. Analysis of the Electric Vehicle Industry Creating the Clean Energy Economy. *International Economic Development Council*, pp. 1–100
- Wen, R., 2012. *Nanostructured $\text{Li}_4\text{Ti}_5\text{O}_{12}$ as Anode Material for Lithium Ion Batteries*. M.Sc. Thesis, Faculty of Science, The University of New South Wales
- Yoshikawa, D., Kadoma, Y., Kim, J., Ui, K., Kumagai, N., Kitamura, N., Idemoto, Y., 2010. Spray-drying Synthesized Lithium-excess $\text{Li}_{(4+x)}\text{Ti}_{(5-x)}\text{O}_{(12-d)}$ and its Electrochemical Property as Negative Electrode Material for Li-ion Batteries. *Electrochimica Acta*, Volume 55(6), pp. 1872–1879
- Young, D., Ransil, A., Amin, R., Li, Z., Chiang, Y.-M., 2013. Electronic Conductivity in the $\text{Li}_{4/3}\text{Ti}_{5/3}\text{O}_4$ - $\text{Li}_{7/3}\text{Ti}_{5/3}\text{O}_4$ System and Variation with State-of-Charge as a Li Battery Anode. *Advanced Energy Materials*, Volume 3(9), pp. 1125–1129
- Zhang, C., Zhang, Y., Wang, J., Wang, D., He, D., Xia, Y., 2013. $\text{Li}_4\text{Ti}_5\text{O}_{12}$ Prepared by a Modified Citric Acid Sol-gel Method for Lithium-ion Battery. *Journal of Power Sources*, Volume 236, pp. 118–125